DETECTION AND ESTIMATION OF WAKE VORTEX ON ULTRA FAST-SCANNING PULSED-DOPPLER LIDAR

Eiichi Yoshikawa*, and Naoki Matayoshi*
*Japan Aerospace Exploration Agency

Abstract

An algorithm for the detection and estimation of a wake vortex using a lateral Range Height Indicator (RHI) observation of a pulsed-Doppler lidar is proposed. By estimating physical parameters from measured Doppler spectra, the proposed method achieves high accuracy and robustness even in low Carrier-to-Noise Ratio (CNR) conditions. This paper describes the methodology and presents an initial evaluation with data collected in a wake vortex observation campaign at Narita Airport, Japan.

1 Introduction

Wake vortex is one of critical issues in reducing aircraft separation distances and increasing airport capacity [1]. The Japan Aerospace Exploration Agency (JAXA) has started a wake vortex observation campaign using a lidar at Narita airport (Tokyo Metropolitan Airport) in order to obtain knowledge of wake vortex behaviors in various weather conditions to allow a reduction of aircraft separation without loss of safety [2], [3], [4], [5], [6].

Multiple continuous wave (CW) lidars have been utilized to observe wake vortices to learn their behaviors because this approach enables wake vortex physical parameters to be estimated accurately [2]. Since a CW lidar does not have a ranging capability, two or more CW lidars share one vertical cross-section, and elevations indicating a wake vortex from the two lidars are combined to determine the position of the wake vortex in the cross section. Because a transmitted laser beam is sharp and of negligible width, the position of a wake vortex

is detected precisely. However, this approach focuses on wake vortices in a limited small area, and is sensitive to the positional relationships between wake vortices and lidars, and to obstacles around the lidars.

On the other hand, a pulsed-Doppler system accomplishes the detection and estimation of wake vortices in a wide area. A Range Height Indicator (RHI) observation by a single pulsed-Doppler lidar system can detect and estimate wake vortices by its ranging capability. Although pulsed-Doppler lidars generally output the first three moments (zeroth, first, and second moments) of Doppler spectra, the measured Doppler spectra themselves are necessary to accurately estimate wake vortex parameters because aircraft wake vortices typically have a small spatial structure, with core radii of less than 10 m, compared to the laser pulse length which is at least tens of meters with current technology. K. Friedrich *et al.* proposed an algorithm to estimate wake vortices from the Doppler spectra measured by a pulsed-Doppler lidar [7]. Specifically, this algorithm uses the two spectral components that correspond to the minimum and maximum velocities in each resolution volume from among the spectral components with sufficient received power level. The algorithm has shown good agreement with estimates obtained using Multiple CW lidars.

A problem with lidars is that the received laser power greatly depends on atmospheric conditions. Moreover, the power of the signal received by a pulsed-Doppler system is generally less than that received by a CW system, because the emitted energy is equivalent to the time integral of the emitted power and a pulsed-Doppler lidar must emit short-duration

pulses to achieve high range resolution. It is therefore impractical to apply the method of detecting minimum and maximum velocity components to estimate wake vortex parameters since it is difficult to obtain those two received signal components with sufficient power in other than high aerosol density conditions.

In this paper, we propose an algorithm to detect and estimate wake vortex parameters using a pulsed-Doppler lidar which achieves both accuracy and robustness (high estimation accuracy even in poor atmospheric conditions for practical use). The algorithm is developed based on four key ideas: (1) Processing of all measured Doppler spectra components in range-angle bins around the center of a wake vortex to extract structures smaller than the physical range resolution, (2) Use of a presupposed two-dimensional vortex model to characterize the wake vortex using a small number of parameters, (3) Design of a cost function to optimize the wake vortex parameters to fit the measured Doppler spectra on Bayesian scheme, taking into account the probabilistic properties of lidar signals to cover cases with low received power, and (4) Use of iterative optimization to reach a minimum cost in the non-linear relationship between the wake vortex parameters and the measured Doppler spectra. Section 2 gives a background of lidar observations and section 3 elaborates the proposed algorithm in further detail. An example of an estimation result by applying the proposed algorithm to lidar data acquired in our observation campaign at Narita airport is shown in section 4, along with statistical evaluation of the proposed algorithm using data collected between November 2013 and February 2014. Section 5 concludes the paper.

2 Background

A pulsed-Doppler lidar radiates pulsed laser light into the atmosphere. Emitted pulses are intercepted and scattered by aerosol particles that move with the airflow, and back-scattered radiation is received by the lidar. The round-trip time from pulse emission to the reception of backscattered light from a particle gives its range, and the shift of frequency of the received

radiation due to the motion of the particle in the pulse axis direction gives its speed in that direction. In practice, a lidar receives the sum of the signals from all aerosol particles inside the resolution volume defined by the round-trip time, the pulse length, and the sharpness of the emitted beam. Thus, the Doppler spectrum in a resolution volume calculated by Fourier transforming a received time-domain signal has a broadened spectral shape that expresses the various lidar-radial velocities of each aerosol particle in the resolution volume. A lidar signal contains white noise which affects all spectral components equally, so spectral components having weaker power (fewer aerosols) than the noise level are not longer available. To gain received power, incoherent integration is generally applied by transmitting several hundreds to several thousands of pulses.

In typical use, a pulsed-Doppler lidar outputs Carrier-to-Noise Ratio (CNR), mean radial velocity, and velocity dispersion, which correspond to the zeroth, first, and second moments of a Doppler spectrum. As is well known, these values can differ from quantities obtained by direct observation using instruments such as anemometers because of two main causes: (1) The resolution volume of current pulsed-Doppler lidars is larger than that of anemometers, and (2) measured Doppler spectra fluctuate probabilistically like other remote sensors. The former implies that to extract small spatial structures such as wake vortices inside a resolution volume, it is not sufficient to use the moments of the measured Doppler spectra but necessary to use components of Doppler spectra themselves. With respect to the latter, it is important to consider the probabilistic characteristics inherent in measured Doppler spectra. The probabilistic properties of Doppler spectrum measurements are described with several assumptions in [8].

3 Methodology

The proposed algorithm is based on and extends the algorithm proposed by R. Frehlich and R. Sharman [9]. The proposed algorithm is an iterative procedure to optimally fit wake vortex parameters to measured Doppler spectra in a
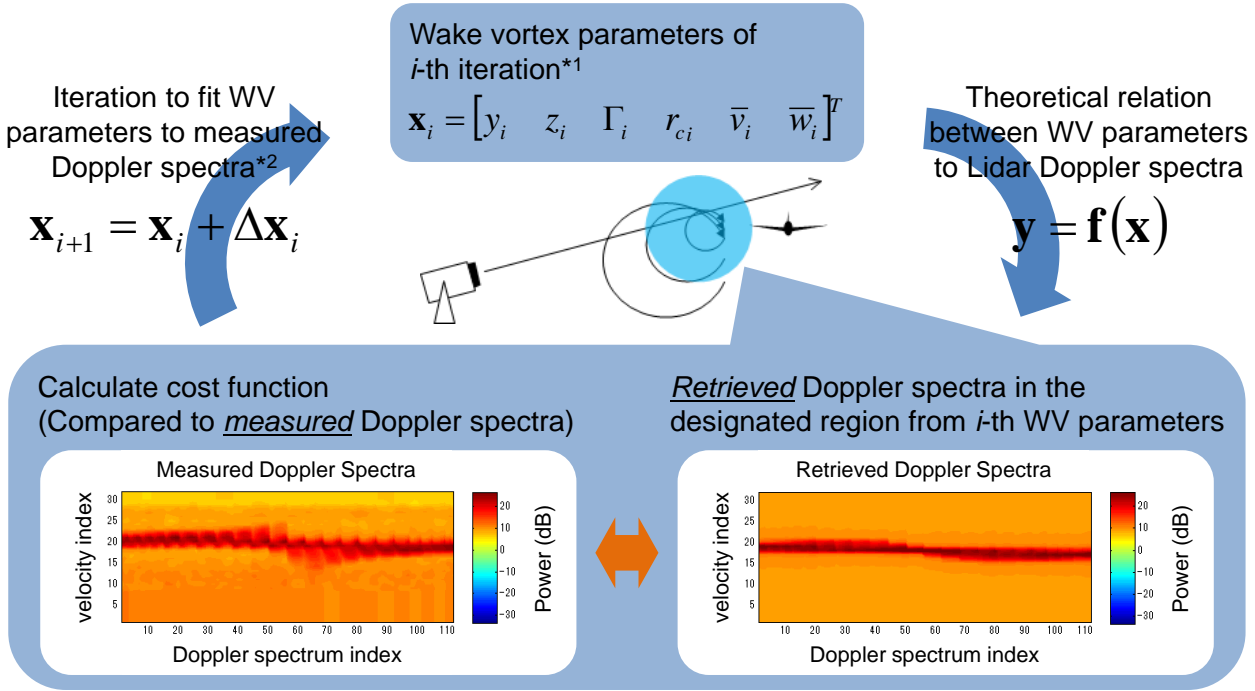
Figure 1 Flow of the proposed algorithm

probabilistic sense. As a premise, it is supposed that a pulsed-Doppler lidar is operated in an RHI observation mode. Applying a 2-D wake vortex model, a vector of state variables is defined as

$$\mathbf{x} = \begin{bmatrix} y & z & \Gamma & r_c & v_b & w_b \end{bmatrix}^T . \quad (1)$$

These state variables are assumed to be valid within an area less than a specified distance from the vortex center. y and z are the horizontal range and height of the vortex center from the lidar, and v_b and w_b are the horizontal and vertical background wind velocities. That is, the background wind is assumed to be constant within the defined area. Γ and r_c are the parameters of the assumed 2-D vortex model, such as the Rankine, Lamb-Oseen, or Hallock-Burnham models. For example, the Hallock-Burnham model is expressed as

$$v_\theta = \frac{\Gamma}{2\pi r} \frac{r^2}{r^2 + r_c^2} . \quad (2)$$

where v_θ is the vortex tangential velocity. The $\mathbf{x}$ vector may include more variables in order to apply a vortex model with more variables or to express the background wind more precisely. The main difference from the Frehlich and Sharman's algorithm is that the $\mathbf{x}$ vector includes the background wind elements.

Although they assumed that the background wind is known, it is frequently difficult to estimate background wind in our RHI observation, which is mentioned in the next section.

The vector of state variables, $\mathbf{x}$, is translated to Doppler spectra retrieved from the designated area. First, the 2-D wind velocity field in the RHI plane is calculated by tangential wind velocities determined by the vortex model parameters and background wind velocities. The 2-D wind velocity field is projected onto the lidar radial wind velocity field in a simple trigonometric manner. Doppler spectra in the designated area are retrieved by accumulating Doppler spectra in small parts of the resolution volume. It is assumed that aerosols uniformly fill the resolution volume with a constant turbulence. The relationship between the state variables and the retrieved Doppler spectra is then expressed as

$$\mathbf{y} = \mathbf{f}(\mathbf{x}), \quad (3)$$

where $\mathbf{y}$ consists of all components of the Doppler spectrum of all the resolution volumes in the designated area and $\mathbf{f}(\mathbf{x})$ is a non-linear theoretical relationship between the wake vortex parameters and the lidar Doppler spectra. Thus, when there are m resolution volumes in the

Table 1 Lidar specifications

Lidar	
Type	Pulsed-Doppler
Wavelength	1543 nm
Physical range resolution	25, 50, 75, and 100 m
Range gate interval	1 m (minimum) with range overlapping
Number of range gates	240 (max)
Azimuth angle	0 – 360 deg
Elevation angle	-10 – 190 deg
Angular resolution	0.1 deg
Pointing accuracy	0.1 deg
Radial wind speed	-30 – 30 m/sec
Measurements	CNR, radial velocity, velocity dispersion, Doppler spectrum, range, gazing angle, and time.
Observation modes	Plan Positioning Indicator (PPI), Range Height Indicator (RHI), Doppler Beam Swinging (DBS), and Line Of Site (LOS)
Weight	232 kg
Size (H-W-D)	1365-1008-814 mm
Power consumption	500 – 1600 W
Rapid RHI	
Range sampling	Every 5 m from 100 – 885 m for landing aircrafts, and from 200 – 985 for take-off aircrafts
Physical range resolution	About 50 m
Elevation sampling	Every 0.2 deg from 0 – 40 deg for landing aircrafts, and from 20 – 60 deg for take-off aircrafts
Velocity sampling	Every 3 m/sec from -30 – 30 m/sec
Pulse repetition	18,000 Hz
Number of accumulated pulses	600
Scan duration	6.7 sec (+2 sec to reset scanner head)

defined area and each Doppler spectrum has n components, $\mathbf{y}$ is a vector with $m \times n$ elements.

Based on a probabilistic property of a measured Doppler spectrum [8], it is assumed that a component of a Doppler spectrum has fluctuation with a Gaussian distribution of which the mean is the received power of the component and the standard deviation is also determined by the received power. With this known probabilistic property, an optimum

solution of $\mathbf{x}$ is calculated in a Bayesian scheme by minimizing the cost function

$$J(\mathbf{x}) = \sum_{k=1}^{m \times n} \frac{(y_k - \hat{y}_k)^2}{\sigma_k^2}, \qquad (4)$$

where y_k is a retrieved Doppler spectral component, $\hat{y}_k$ is a measured Doppler spectral component, and σ_k is the standard deviation of the known probabilistic property.

Figure 1 shows the flow of the iterative process to minimize Eq. (4) and reach the optimum $\mathbf{x}$. First, an initial solution of $\mathbf{x}$ is calculated by a first moment-based method. A pair of positive and negative radial velocities is detected by thresholding range and velocity differences between the two, then y and z are determined. Γ and r_c are calculated by radial velocities agreeing with tangential direction of the wake vortex. v_b and w_b are set to 0. From the initial $\mathbf{x}$, Doppler spectra in resolution volumes inside the designated area are retrieved. By comparing the retrieved and measured Doppler spectra, the innovation factor of $\mathbf{x}$, $\Delta\mathbf{x}$, can be determined by a general optimization procedure, and $\mathbf{x}$ is updated with less cost. Applying this process iteratively allows $\mathbf{x}$ to reach the optimal solution. In this paper, a published algorithm, the BOBYQA subroutine proposed by M. J. D. Powell [10], is applied as the optimization procedure, which is based on quadratic approximation to calculate the innovation factor.

4 Estimation Result

As stated previously, JAXA is conducting a wake vortex observation campaign using an ultra fast-scanning lidar. The specifications of the lidar and its operation mode are summarized in Table 1. The lidar, a Leosphere WINDCUBE200S, radiates 1543 nm laser pulses whose physical lengths are almost 50 m. Light backscattered from aerosols flowing with air are received and digitally sampled. For each orientation of the scanning head, data for 600 pulses at a pulse repetition frequency of 18 kHz are processed and accumulated, and measurements of Carrier-to-Noise Ratio (CNR), mean radial velocity, velocity dispersion, and Doppler spectrum are output for 5 m range bins
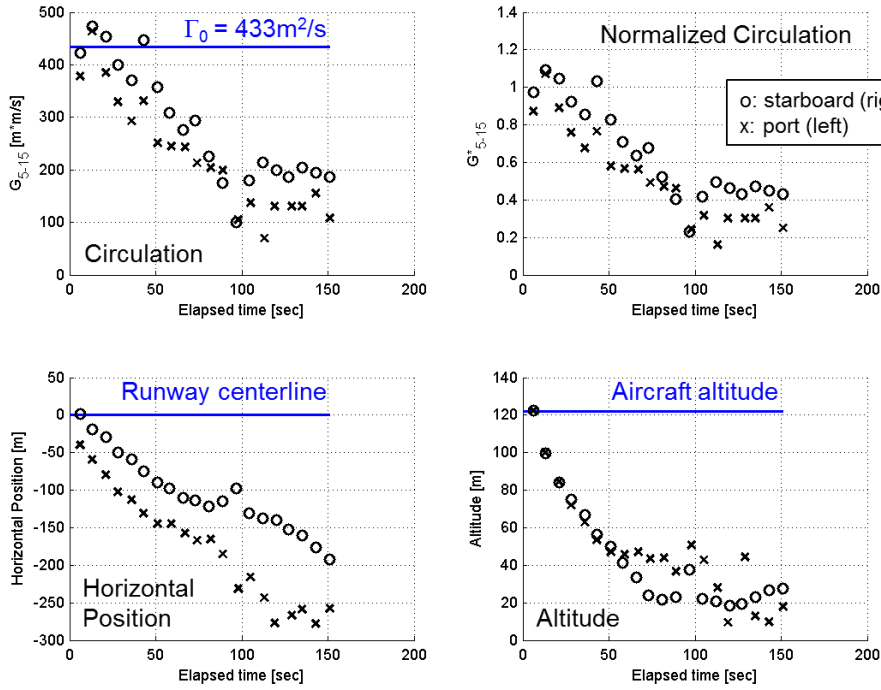
Figure 2 An example of estimated wake vortex behavior

to almost 900 m. In one RHI plane, range profiles are obtained at elevation angles up to 40 deg in 0.2 deg increments. The scan duration of one RHI is 6.7 sec, and almost two further seconds are needed to reposition the scanner head for the start of the next RHI. Due to the rapid RHI scan, the temporal evolution of a wake vortex in a single RHI is almost negligible, and successive 2-D structures are obtained with a short time interval between them. In the proposed algorithm, the Hallock-Burnham model is assumed, and the **x** vector is valid 20 m from the vortex center. An RHI mode with such low elevations is necessary in order to observe the wake vortex complex behavior at low altitudes. The reason why the **x** vector needs to include the background wind element is because it is difficult to estimate background wind with such a narrow range of elevation, and horizontal wind has a large vertical gradient due to ground effect.

An example of wake vortex behavior is shown in Figure 2. The upper left and upper right plots show the time histories of circulation and normalized circulation, respectively. A set of circulation and core radius estimated by the

proposed algorithm is converted to a radii-averaged circulation from 5 to 15 m from the center of a wake vortex, $\Gamma_{m,}$ based on the assumed vortex model. The lower left and lower right plots show those of horizontal range from the centerline of the runway the aircraft landing to and altitude. In each plot, circles and x symbols indicate lidar port and starboard wake vortices, respectively. In this case, a wake vortex behavior is traced up to about 150 sec elapsed time. From the generation of the vortex to its decay to a circulation of $100 - 200$ m^2/sec after 100 sec elapsed, the wake vortex behavior is well resolved at the short time intervals of 8 sec. Horizontal range and altitude are also estimated with high temporal resolution. In the observation campaign, Quick Access Recorder (QAR) data from aircraft whose wake vortices were observed by the lidar are obtained to evaluate the proposed algorithm. The QAR data include the position at which the aircraft pass the RHI plane, and derive the root circulation of the two generated wake vortices as,

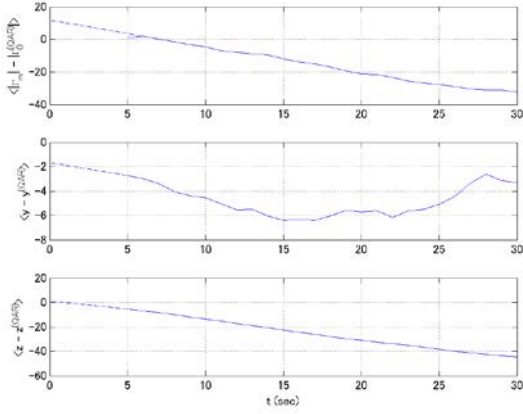$$\Gamma_0 = \frac{Mg}{\rho s B V}, \tag{5}$$

Figure 3 Mean Differences between the proposed algorithm and the reference values from the QAR data

Figure 4 Standard deviations between the proposed algorithm and the reference values from the QAR data ($\sigma_{Q\text{-}L}$)

Figure 5 Standard deviations by the self-evaluation ($\sigma_{L\text{-}L}$)

where M is mass of aircraft, g is the acceleration due to gravity, ρ is the air density, s is the spanwise load factor (assumed as $\pi/4$ in this paper), B is the aircraft wing span of aircraft, and V is airspeed of aircraft. The reference values indicated in the upper left, lower left, and lower right plots are derived from the QAR data. And, the root circulation of 433 m²/sec is used in the normalization for the upper right plot.

Cross validation by comparing horizontal range, height, and mean circulation estimated by the proposed method with values derived from the QAR data clarify the estimation accuracy of the proposed method. Here, only estimated parameters of 1,341 pairs of wake vortices until an elapsed time of 30 sec are evaluated because the QAR data provides parameters of a wake vortex which just generated (t = 0 sec). Mean difference between time histories of the estimated wake vortex parameters and the reference values from the QAR data are shown in Figure 3, where the upper, middle, and lower plots correspond to circulation, horizontal range, and height, respectively. The dashed lines are linear extrapolations to t = 0 sec. The upper plot shows that the difference of circulation is monotonically decreasing due to the decay process except for that in t = 5 sec. The bias error of circulation is estimated about +15 m²/sec when the circulation in t = 5 sec is neglected. The middle and lower plots indicate that bias errors of the location of the proposed algorithm are roughly few meters. The standard
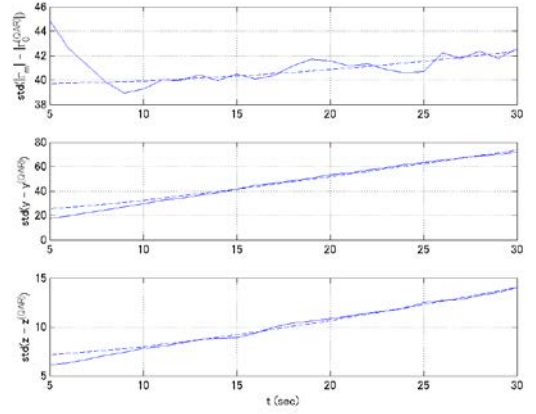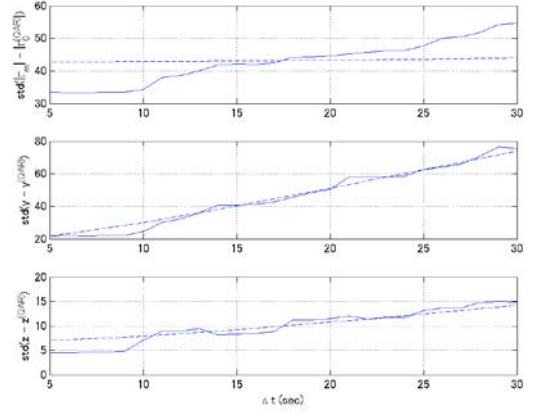
deviation of differences between the two is assumed as

$$\sigma^{(x)}{}_{Q-L}\left(t\right)^2 = \sigma^{(x)}{}_{est}{}^2 + \sigma^{(x)}{}_{gen}{}^2 + \left(t\sigma^{(x)}{}_{prg}\right)^2, \quad (6)$$

where $\sigma_{Q\text{-}L}$ is the standard deviation between the values determined by the proposed method and the QAR-derived values, σ_{est}, σ_{gen}, and σ_{prg} are standard errors due to the proposed method, due to generation process of a wake vortex (error of Eq. (5)), and due to temporal progress of a wake vortex, respectively, and t is the elapsed time from the vortex generation. The superscript (x) denotes an evaluated wake vortex parameter, y, z, or Γ_m. At the same time, an equation of self-evaluation is also expressed as

Table 2 Estimation accuracy of the proposed method evaluated with the QAR data

Wake vortex parameter	σ_{est}	σ_{gen}	σ_{prg}
Mean circulation, Γ_m (m^2/sec)	30.2 – 40.6	– 27.1	0.3
Horizontal range, y (m)	13.0 – 19.1	– 14.0	2.4
Height, z (m)	4.8 – 6.5	– 4.4	0.4

$$\sigma^{(x)}{}_{L-L}\left(\Delta t\right)^2$$
$$= n\sigma^{(x)}{}_{est}{}^2 + \left(\Delta t\sigma^{(x)}{}_{prg}\right)^2, \qquad (7)$$

where σ_{L-L} is the standard deviation between two estimation results of the same wake vortices from two RHI scans at different times, Δt is the time difference between the two RHI scans, and n expresses the dependency between the two estimations (that is, $n = 2$ if the two estimations are independent). Although a strict evaluation requires more samples of obtained data, a rough estimate of accuracy is calculated. That is, the possible worst σ_{est} is calculated by solving Eq. (6) assuming $\sigma_{gen} = 0$, and the possible best σ_{est} is calculated by Eq. (7) assuming $n = 2$. In Figure 4, the standard deviations of the difference between values from the proposed algorithm and of the QAR are shown. In the upper plot corresponding to circulation, decrease in the first ten seconds does not agree with the assumption of Eq. (6). This large standard deviation indicates that there is a large uncertainty in generation of a wake vortex. Evaluation by Eq. (6) except for the first ten seconds derives $40.6\,\text{m}^2$/sec as the possible worst σ_{est} of circulation. In horizontal range and height, which are shown in the middle and lower plots, the worst σ_{est} is 19.1 m and 6.5 m, respectively. At the same time, σ_{prg} of them are calculated as $0.3\,\text{m}^2$/sec, 2.4 m, and 0.4 m. Dashed lines of each plot are σ_{Q-L} retrieved from these derived values, which are well agreed after an elapsed time of 10 sec. In Figure 5, results of the self-evaluation by Eq. (7) are shown. Here, σ_{prg} derived by Eq. (6) are substituted to Eq. (7). As stated above, when $n = 2$, the possible best σ_{est} are calculated as $30.2\,\text{m}^2$/sec, 13.0 m, and 4.8 m. As in Figure 4, retrieved σ_{L-L} is expressed by dashed lines. Although the good agreements in horizontal range and height, the retrieved line of circulation is much different from the original line drawn by solid line. This is probably

because coefficient n is time-dependent due to correlation between two estimated circulations whose Δt is small. It will be clarified by further analyses with a larger number of data. The standard deviations calculated in this section, are summarized in Table 2.

5 Conclusion

This paper proposes an algorithm for the detection and estimation of a wake vortex on a lateral RHI observation of a pulsed-Doppler lidar is proposed. The traditional method using multiple CW lidars can estimate physical parameters of a wake vortex only in a limited small area and is sensitive to the positional relationships between a wake vortex and lidars and to surrounding obstacles. Our proposed method uses a single pulsed-Doppler lidar without those drawbacks. Moreover, compared with a first moment-based method and a method using two spectral components with maximum and minimum velocities, the proposed method extracts smaller structures of a wake vortex with more robustness for any CNR conditions. As described in [1], our wake vortex observation campaign is ongoing. In the next step, estimation accuracy will be evaluated with all the data collected from this observation campaign. Although only standard deviation is mentioned in this paper, bias errors of the proposed method will also be evaluated through lidar signal simulations. After these evaluations, the estimated wake vortex behaviors (time evolution of wake vortex parameters) will be utilized to develop a probabilistic wake vortex prediction model to enable safe reduced wake vortex separation minima.

References

[1] Yoshikawa, E., and Matayoshi, N., "Wake Vortex Observation Campaign by Ultra Fast-Scanning Lidar

in Narita Airport, Japan," 29th Congress of the International Council of the Aeronautical Sciences (ICAS), Sept., 2014, St. Petersburg, Russia (in printing).

[2] Gerz, T., Holzäpfel, F. and Darracq, D., "Aircraft Wake Vortices: A Position Paper," Wakenet, 2001.

[3] WakeNet2-Europe, "Wake Vortex Research Needs for 'Improved Wake Vortex Separation Ruling' and 'Reduced Wake Signatures'," Final Report of the Thematic Network 'WakeNet2-Europe', 6th Framework Program, National Aerospace Laboratory, NLR-CR-2006-171, April, 2006.

[4] Barbaresco, F., Brovelli, P., Currier, P., Garrouste, O., Klein, M., Juge, P., Ricci, Y., and Schneider, J.-Y., "Radar Sensor for Wind & Wake-Vortex Monitoring on Airport: First results of SESAR P12.2.2 XP0 trials campaign at Paris CDG airport", proceeding of the seventh European conference on radar in meteorology and hydrology (ERAD 2012), Toulouse, Jun., 2012.

[5] Barbaresco, F., Juge, P., Klein, M., Ricci, Y., Schneider, J.-Y., and Moneuse, J.-F., "Optimising Runway Throughput through Wake Vortex Detection, Prediction and Decision Support Tools", proceeding of ESAV'11 Conference (Enhanced Surveillance of Aircraft and Vehicles), Capri, Sep., 2011.

[6] Harigae, M., "Research Plan of DREAMS Project for a Next Generation Operation System", proceedings of the 49th Aircraft Symposium, Kanazawa, Oct., 2011, in Japanese.

[7] Friedrich, K., Stephan, R., and Igor, S., "Characterization of Aircraft Wake Vortices by 2-µm Pulsed Doppler Lidar", Journal of Atmospheric and Oceanic Technology, vol. 21, 2004.

[8] Bringi, V. N., and V. Chandrasekar, "Polarimetric Doppler Weather Radar: Principles and Applications," Cambridge University Press, 2001.

[9] Frehlich, R., and Sharman, R., "Maximum Likelihood Estimates of Vortex Parameters from Simulated Coherent Doppler Lidar Data," Journal of Atmospheric and Oceanic Technology, vol. 22, 2005

[10] Powell, M. D. J., "The BOBYQA algorithm for bound constrained optimization without derivatives", Cambridge NA Report, 2009.

Contact Author Email Address

yoshikawa.eiichi@jaxa.jp

Copyright Statement